BMC Microbiology

RESEARCH Open Access

Analysis of virulence of the emerging opportunistic human pathogen *Achromobacter* in a zebrafish embryo model

Giulia Maria Saitta[1], Julien Boyer[2], Qiman Ma[2,3], Angela Sandri[1], Erika Aparecida Oliveira[2,4], Marzia Boaretti[1], Paola Melotti[5,6], David O'Callaghan[2], Maria del Mar Lleò[1], Caterina Signoretto[1*] and Annette Caroline Vergunst[2*]

Abstract

Background *Achromobacter* spp. are emerging opportunistic pathogens of concern in people with cystic fibrosis (CF) and immunocompromised individuals. These bacteria are known for their intrinsic antibiotic resistance and ability to evade host immune defences. A more comprehensive understanding of the direct interaction between *Achromobacter* spp. and the host innate immune system is necessary for the development of effective intervention strategies. In this study, we used zebrafish embryos to investigate the pathogenic potential of a panel of clinical *Achromobacter* spp. isolates and analysed their interaction with the host innate immune system.

Results Seven CF isolates previously shown to cause distinct levels of cytotoxicity in cell culture, and virulence and inflammation in *Galleria mellonella* larvae and mice, respectively, were analysed in a zebrafish embryo model. One strain caused significant host mortality (87.5%) in zebrafish embryos by 4 days post intravenous injection. Mortality was associated with a strong increase in bacterial load and increased pro-inflammatory cytokine gene expression. Three strains were moderately virulent and induced 8.4 to 12.5% host mortality, with surviving embryos having a constant bacterial load until 4 days post infection, indicating bacterial persistence. The remaining three isolates persisted, but caused less than 3% mortality, and were cleared by 27% of infected embryos, which was associated with minimal induction of pro-inflammatory gene expression at 1 day post infection. To elucidate the role of macrophages, macrophage-depleted embryos were compared with macrophage-proficient embryos after infection with the least virulent strain (0% mortality). The absence of macrophages led to a strong increase in bacterial load and 34% mortality within 4 days, demonstrating a significant role for macrophages in controlling bacterial growth and limiting infection severity. Real time analysis revealed, however, that some isolates were able to survive and replicate in macrophages, thereby contributing to either persistent or pro-inflammatory infection. These results demonstrated both host-detrimental and host-beneficial roles for macrophages during infection.

Conclusion Zebrafish embryos represent a valuable model for studying *Achromobacter*-host interactions during both persistent and acute infection, particularly to study the role of immune cells and obtain insights into host-

*Correspondence:
Caterina Signoretto
caterina.signoretto@univr.it
Annette Caroline Vergunst
annette.vergunst@umontpellier.fr

Full list of author information is available at the end of the article

pathogen interactions in real-time. The zebrafish infection model will be a helpful tool for the discovery antimicrobial strategies against *Achromobacter* spp. infections.

Keywords *Achromobacter* spp, Bacterial virulence, Zebrafish model, Persistence, Pathogenicity, Cystic fibrosis

Background

Bacteria belonging to the genus *Achromobacter* are commonly found in various natural environments. They are emerging opportunistic pathogens of humans, and are known to cause nosocomial infections, including pneumonia, bacteraemia and urinary tract infections, particularly in immunocompromised individuals [1, 2]. Notably, people with cystic fibrosis (CF) are vulnerable to infection with *Achromobacter* spp., where these bacteria can cause severe chronic infections that lead to lung inflammation, an increased frequency of exacerbations, and a decline in respiratory function [3–5]. CF is characterised by a chronic inflammatory state in the lungs, with immune cells such as neutrophils, macrophages, and lymphocytes playing a central role in both defence and tissue damage. While neutrophils are considered the main immune players, macrophages have been shown to have an important role in modulating the immune response, initiating phagocytosis of pathogens and secreting pro-inflammatory cytokines including IL-1β and TNF-α [6]. Infections by *Achromobacter* spp. in CF further exacerbate this inflammatory state. The ability of *Achromobacter* spp. to establish persistent infections has been attributed to their capability to evade host immune defences through the formation of biofilms, and their intrinsic antibiotic resistance which further complicates treatment [7]. In addition, *Achromobacter* spp. have been demonstrated to survive in cultured cells, including human macrophage-like THP-1 cells [8], suggesting that macrophages could provide an intracellular niche that helps the bacteria evade antibacterial treatments. However, the contribution of the intracellular survival of bacteria to infection in vivo has not yet been described.

Several virulence factors that contribute to disease severity have been identified in *Achromobacter* spp. These include colicin V, proteases, cell surface factors such as the Vi capsular polysaccharide and O-antigen, an anti-sigma-E factor, and type 3 and 6 secretion systems [9–12]. Different *Achromobacter* spp. isolates have been shown to cause distinct levels of type 3 secretion system (T3SS)-dependent host cell death by triggering pyroptosis, allowing the bacteria to escape from infected cells after initial intracellular survival in a membrane-bound vacuole [8, 12, 13]. The T3SS effector AxoU and the ArtA RTX adhesin have been identified as essential for cytotoxicity in *Achromobacter xylosoxidans* [12, 13]. However, these bacterial factors are not solely responsible for cytotoxicity, since A*chromobacter insuavis*, which lacks AxoU and the ArtA RTX adhesin, is equally cytotoxic showing that other bacterial factors are involved in this process [8]. In addition, analysis of an *A. xylosoxidans* strain that caused low cytotoxicity revealed bacterial survival in LAMP-1-positive phagosomes in a T3SS-independent manner for at least 24 h. A functional T3SS was, however, required for inflammation in an acute infection model in mice and in *Galleria mellonella* larvae [8].

Although not much is known yet about host inflammatory responses in response to infection with *Achromobacter* spp., pro-inflammatory mediators such as CXCL-8 are released in in vitro cell infections [8]. CXCL-8 plays a major role in the recruitment of neutrophils, and CXCL-8-mediated inflammatory responses to *Achromobacter* spp. infection were observed in vivo in CFTR-knockout mice [14]. Elias-Oliveira and colleagues also reported that intense pulmonary inflammatory responses upon inoculation with *A. xylosoxidans* resulted in fatal infections in mice that depended on CD14 activation as a result of the detection of bacterial lipopolysaccharides [15]. To develop effective treatments, more research is needed to better understand the direct interaction between *Achromobacter* spp. and the host innate immune system, and to increase our knowledge of pathogenicity among different *Achromobacter* species and the virulence of individual isolates.

Zebrafish embryos are a powerful model for studying host-pathogen interactions because of their external development, optical transparency, genetic tractability, and the high similarity of their innate immune system to that of humans. In particular, the optical transparency of zebrafish embryos allows for high-resolution non-invasive live imaging. This makes it possible to observe in vivo interactions between pathogens and host immune cells and track the intracellular fate of bacteria in macrophages in real time using transgenic zebrafish with cell-specific fluorescent reporter proteins. Due to these unique advantages, researchers have developed infection models to investigate the pathogenicity of diverse bacterial, viral and parasitic species [16–18], including important CF pathogens such as *Pseudomonas aeruginosa*, *Staphylococcus aureus* and *Burkholderia cenocepacia* [19–21].

The aim of this study was to establish and validate a zebrafish embryo infection model to assess pathogenicity and real-time interactions of *Achromobacter* with innate immune cells, and to determine a more precise role for macrophages during infection. Previously, we analysed several CF isolates for virulence in *G. mellonella* larvae, cytotoxicity in wildtype (WT) and CF (F508del) human

bronchial epithelial cells, and lung inflammation in wild-type and CFTR-knockout mice [14]. The present study investigated the virulence of these same clinical isolates in zebrafish embryos, and revealed infection phenotypes ranging from acute and rapidly fatal to persistent non-fatal, in agreement with the published infection outcomes for these strains in *G. mellonella* larvae and mice. In addition, we demonstrated a dual role for macrophages in dampening the infection and providing an intracellular niche for the bacteria. Zebrafish embryos provide an attractive model for studying the pathogenicity of *Achromobacter* spp. to explore host-pathogen interactions at the interface of the innate immune system, analyse the importance of an intracellular macrophage stage during infection, identify targets for the development of new therapeutic interventions, and study the efficacy of antimicrobial treatments.

Materials and methods

Zebrafish maintenance

The zebrafish used in this study were wildtype AB and the transgenic zebrafish lines Tg(*mpx: eGFP*)^{i114} [22], which expresses GFP in neutrophils, and Tg(*mpeg1:eGFP-caax*)^{gl22} [23], which expresses GFP in macrophages. AB eggs were acquired from the Zebrafish International Resource Center and raised into adult hood to serve as progenitors. Tg(*mpx: eGFP*)^{i114} and Tg(*mpeg1:eGFP-caax*) ^{gl22} were originally obtained from S. Renshaw (University of Sheffield) and G. Lutfalla (University of Montpellier) and maintained in our facility. Zebrafish (*Danio rerio*) were raised, maintained and handled according to the European Union guidelines for laboratory animals. Adult zebrafish were kept in conditioned water (pH: 7.5, conductivity: 650 µS/cm) at 28 °C with a light/dark cycle of 14/10 h. Embryos were collected after light onset from natural spawning.

Bacterial strains and plasmids

The seven *Achromobacter* spp. clinical isolates (see Table 2 for the different species) were collected from the sputum samples of seven patients at the CF Centre of Verona, Italy, and classified by whole-genome sequencing and phylogenetic analysis in previous studies [10, 24]. The bacterial strains were stored in Microbank (Pro-Lab Diagnostics, Neston, UK) at – 80 °C. Bacteria were electroporated with plasmid pIN29 encoding chloramphenicol acetyl transferase (CAT), providing resistance to chloramphenicol, and the fluorescent protein DsRed, using conditions described earlier for *B. cenocepacia* [25, 26]. Plasmid-containing bacteria were selected on LB agar supplemented with 100 mg/L chloramphenicol (Cm100). The presence of the plasmid did not negatively impact the fitness of the strains, and the plasmids were stably maintained in the absence of antibiotic selection pressure during 72 h of infection, with less than 5% of bacteria that had lost DSRed fluorescence.

Zebrafish embryo infection

Microinjection of bacteria in zebrafish embryos was carried out as previously described [26]. Bacteria were collected from overnight cultures, adjusted to an OD_{600} of 1, and centrifuged at 3,000 × g for 2 min. The pellet was subsequently resuspended in phosphate-buffered saline (PBS). Bacterial dilutions were made in PBS and 0.05% phenol red was added to visualise microinjection. The embryos were manually dechorionated 2 h before injection. Embryos were staged at 30 h post-fertilisation (hpf), anaesthetised in E3 medium supplemented with 0.04% buffered MS222 (tricaine; ethyl-3-aminobenzoate methanesulfonate salt; Sigma) and intravenously microinjected with 1 nL of inoculum corresponding to on average 500 colony forming units (CFU), using a Femtojet microinjector (Eppendorf) and a micromanipulator with pulled micro-capillary pipettes. Due to small differences in injection volume between injection needles, the precise inoculum size for each strain was determined by injecting directly into a 100 µL drop of PBS (n = 3) that was then evenly spread onto LB agar (1.5%). Precise CFUs are indicated for each experiment in the respective legends. After injection, the embryos in each group were washed in E3 medium, randomized and each embryo was individually transferred to 0.5 mL of E3 medium in 48-well plates. The embryos were placed in an incubator at 28 °C and with a 14/10 h light (combination of cold white and warm white light LEDs)/dark regime. For each strain, one 48 well-plate was used for CFU counts (n = 5 individual embryos per experiment per time point), the second was used for monitoring survival once daily, for up to 4 days post-injection (n = 24 per experiment) by determining the presence of a heartbeat. Zebrafish embryos that survived the infection were euthanised in E3 medium containing an overdose of the anaesthetic lidocaine hydrochloride (1 g/L; Sigma), buffered with 2 g/L sodium bicarbonate and mixed with 50 mL/L ethanol, as described [27].

Determination of colony forming units

At 1, 2 and 3 days post-infection (dpi) the bacterial load was determined by plating individually disrupted embryos on LB agar with Cm100 [26]. Briefly, the embryos were rinsed in E3 medium, anesthetised in E3 medium containing 0.02% MS222, individually disrupted with Eppendorf pestles in 1.5 ml tubes containing 100 µL of distilled water, and incubated for 10 min at room temperature. Total lysate and serial dilutions were plated on LB agar plates supplemented with Cm100, and incubated overnight at 37˚ C. The number of colonies was counted the following day. CFU counts for all strains at 1, 2- and

3 dpi were from 5 surviving embryos at each time point while dead embryos were excluded, and may therefore not reflect the variation in bacterial burden at the population level. However, the combination of host survival and bacterial load for a given strain determine the strain's virulence and ability to persist.

Analysis of gene expression by reverse transcriptase (RT)-qPCR

At 3 and 24 h post infection (hpi), embryos were collected for RNA isolation, cDNA synthesis, and qPCR analysis. The peptidylprolyl isomerase A-like (*ppial*) gene was used as the housekeeping gene. A set of immune-related genes (Table 1) was analysed for gene expression changes upon infection. For each condition, 15 embryos were transferred to 500 µL of TRIzol, homogenised with an Eppendorf pestle, vortexed, and stored at -80˚C as previously described [25, 26]. RNA extraction was performed using the Rneasy MinElute Cleanup Kit (Bio-Rad). Reverse transcription of each sample (500 ng total RNA) was carried out using the iScript cDNA synthesis kit (Bio-Rad) following the manufacturer's instructions. Quantitative PCR was conducted using LightCycler® 480 SYBR Green I Master mix kit (Roche) and a LightCycler® 480 (Roche). The primers used are summarised in Table 1. The cycling parameters were: 95˚C for 10 min, followed by 45 cycles of 95˚C for 15 s and 60˚C for 40 s. Fluorescence measurements were taken at the end of each cycle. Melting curve analysis was performed to confirm the absence of primer dimers and nonspecific products. The stability of the housekeeping gene *ppial* was checked for each experiment. The results were analysed using the ΔΔCt method.

Macrophage depletion

Morpholino antisense oligos, designed to block translation and/or splicing of pre-mRNA, were used to knockdown the expression of the Pu.1 transcription factor that is necessary for the differentiation of early myeloid progenitor cells into immune cells [28]. Eggs of Tg(*mpeg1:eGFP-caax*)^{gl22} fish were microinjected at the one-to-four-cell stage with 1 nL of a mixture of tMO_pu.1 (5'-CCTCCATTCTGTACGGATGCAGCA T-3', 0.1 mM) and sMO_E4I5_pu.1 (5'-GGTCTTTCTC CTTACCATGCTCTCC-3', 0.38 mM), which specifically blocks macrophage but not neutrophil development [19, 29]. The eggs were incubated in E3 medium at 28˚C. The absence of GFP-expressing macrophages was validated, prior to injection with bacteria, as described above. Non-injected eggs were used as controls.

Microscopy analysis

For quantification of neutrophils at different time points after infection, Tg(*mpx: eGFP*)^{i114} embryos were transferred to glass-bottom dishes (MatTek Corporation) in E3 containing 0.02% MS222. The embryos were placed on top of 1% agarose/E3 medium in a lateral position ensuring that the trunk was in the same focal plane as the tail region. A Nikon AZ100 multizoom microscope, which was equipped for bright-field and fluorescence imaging and coupled with a Coolsnap HQ2 camera (Roper Scientific), was used to record images of whole embryos with MetaVue software. Images were analysed using the Imaris software (Oxford Instruments, version 10.1.1). The number of neutrophils per image was quantified using the "spot" option.

A Nikon AZ100 and Leica DM IRB inverted microscope, each coupled to a Coolsnap fx camera (Roper Scientific), were used for imaging the progression of the infection in Tg(*mpeg1:eGFP-caax*)^{gl22} embryos injected with DSRed expressing bacteria. For the purpose of imaging bacterial burden in macrophages the inoculum size was reduced to 200 CFU, unless indicated otherwise. An Fv10i confocal laser scanning microscope and Fluoview software (Olympus Life Science) were used to analyse the interaction of bacteria with host immune cells. Some confocal images were further treated with Imaris, by applying the surface structure option.

Statistical analysis

Statistical analysis was performed using GraphPad Prism 10. The results of the survival assays are presented in Kaplan-Meier graphs and analysed with a Log-rank (Mantel-Cox) test. The *P*-values for each pair-wise comparison are indicated in the results section, and significance does not account for multiple comparisons. In

Table 1 Primers used for qRT-PCR experiments

Gene	ENSDARG nb	Forward qPCR primer	Reverse qPCR primer
ppial	ENSDARG00000042247	ACACTGAAACACGGAGGCAAAG	CATCCACAACCTTCCCGAACAC
cxcl8a	ENSDARG00000104795	TGTGTTATTGTTTTCCTGGCATTTC	GCGACAGCGTGGATCTACAG
il1b	ENSDARG00000005419	GAACAGAATGAAGCACATCAAACC	ACGGCACTGAATCCACCAC
cxcl18b	ENSDARG00000075045	TCAAGAGTGGGAATTCTGGG	AGTGATCCGGGTGTTTTCAG
mpeg1	ENSDARG00000055290	GTCTTATATCTCCAACAGTCAG	GATGCCTGGGTAGAATAAAGC
mpx	ENSDARG00000019521	ACCATTGCGAACGTCTTTGC	ACTGGGAAACTGAGGATGGTTC
myd88	ENSDARG00000010169	GATAGTGATGCCTGTGATTTTCAGA	ACGGCCTCTTCATGGATTTGTA
nfkb2	ENSDARG00000038687	CACAGTCTCAGTCGAACTCACAAATA	GCTGTACTGTAATAAAGCACGAGCAT

experiments determining CFU counts, the significance of differences between multiple selected groups was determined using a nonparametric Kruskal-Wallis test with Dunn's multiple comparisons test, since not all the data were normally distributed according to the D'Agostino & Pearson normality test. CFU counts were $\log_{10}$-transformed and presented in dot graphs showing the average per time point, with each dot representing a single embryo. Zero CFU counts were transformed to 1 CFU counts, to be able to include the $\log_{10}$ 0 in the graphs. The significance of the differences in neutrophil counts was determined using a one-way ANOVA with Sidak's multiple comparisons test. RT-qPCR data were $\log_2$-transformed, and significance was analysed using a one-way ANOVA with Sidak's multiple comparison test for each gene by comparing the treatments at each time point with the PBS control and with each other.

Results

Virulence of *Achromobacter* spp. strains in zebrafish embryos

We analysed the virulence of seven *Achromobacter* spp. clinical isolates, including four *A. xylosoxidans*, one *A. agrifaciens*, one *A. insolitus*, and one *Achromobacter* strain with a new genotype (NG), not phylogenetically related to any publicly available sequence [30, 31]. These isolates have been demonstrated previously to have varying levels of cytotoxicity in human bronchial epithelial cells, biofilm formation in vitro, and virulence in *G. mellonella* larvae and mice (summarised in Table 2 [a–d]) [14, 32].

Zebrafish embryos AB were intravenously injected with an average of 500 CFU of each of the 7 clinical isolates of *Achromobacter* spp., and their survival was monitored for 4 days (Fig. 1A, B, Table 2[e]). Isolate 7 – 2 induced rapidly fatal infections in zebrafish embryos, killing 87.5% of the embryos within 4 days, which agreed with high virulence in *G. mellonella* and mice. Infection with the isolates 8 – 2, 17 – 1, 23 – 1 caused between 8.4% and 12.5% mortality at day 4 in zebrafish embryos. Two of these strains (8 – 2 and 23 – 1) showed high virulence in *G. mellonella* and mice, while strain 17 – 1 was less virulent in these models. The remaining three strains (12 – 2, 16 – 1 and 20 – 1), which were previously classified as nonvirulent in *G. mellonella* and mice, induced less than 3% embryo mortality in zebrafish embryos (Fig. 1B). The survival probability of the latter three least virulent strains differed significantly from that of strains 8 – 2 ($P = 0.0316$, $P = 0.0020$, and $P = 0{,}0292$ respectively) and 17 – 1 ($P = 0.0309$, $P = 0.0020$, and $P = 0.0284$, respectively), although no significant differences were found between strain 23 – 1 (causing 8.4% mortality) for any of the 5 strains.

The bacterial load was determined in 5 individual embryos per strain at 1, 2, and 3 dpi. Infection with

Table 2 Overview of the capacity to form biofilms, cytotoxicity, and virulence in *G. mellonella* and mice from previous studies, and in zebrafish embryos in this study, of seven *Achromobacter* isolates

Isolate	*Achromobacter* Species	Biofilm formation in vitro [a]	Cytotoxicity in bronchial epithelial cells [b]	Virulence in *G. mellonella*[c]	Mortality in mice at 4 dpi ($n = 4$) [d]		Mortality in zebrafish embryos at 4 dpi ($n = 75$) [e]
					WT	CF	
7 – 2	*A. xylosoxidans*	Low	Medium	High	75%	100%	87.5%
8 – 2	*A. xylosoxidans*	High	Medium	High	65%	100%	12.5%
12 – 2	*A. agrifaciens*	High	Low	No	0%	25%	2.8%
16 – 1	*Achromobacter NG*	Low	Low	No	0%	0%	0%
17 – 1	*A. xylosoxidans*	High	No	Medium	0%	50%	12.5%
20 – 1	*A. insolitus*	Medium	Medium	No	0%	0%	2.8%
23 – 1	*A. xylosoxidans*	Low	Low	High	25%	65%	8.4%

NG New genogroup

[a] Biofilm formation [32]

[b] Cytotoxicity in bronchial epithelial cells [32]

[c] Virulence in *G. mellonella* (high, > 50% larval death in 24 h; medium, > 50% larval death in 48 h; low, > 50% larval death in 72 h; no, < 50% larval death in 72 h) [32]

[d] Mortality in mice 4 d after intratracheal challenge [14]. WT= wildtype; CF = cystic fibrosis. Mouse data are from a previous study in which 12-week-old congenic C57BL/6NCrlBR (WT) and C57BL/6NCrlBR Cftrtm1UNCTgN(*FABPCFTR*) female mice were used

[e] Mortality in zebrafish embryos at 4 dpi (this study, Fig. 1A and B)

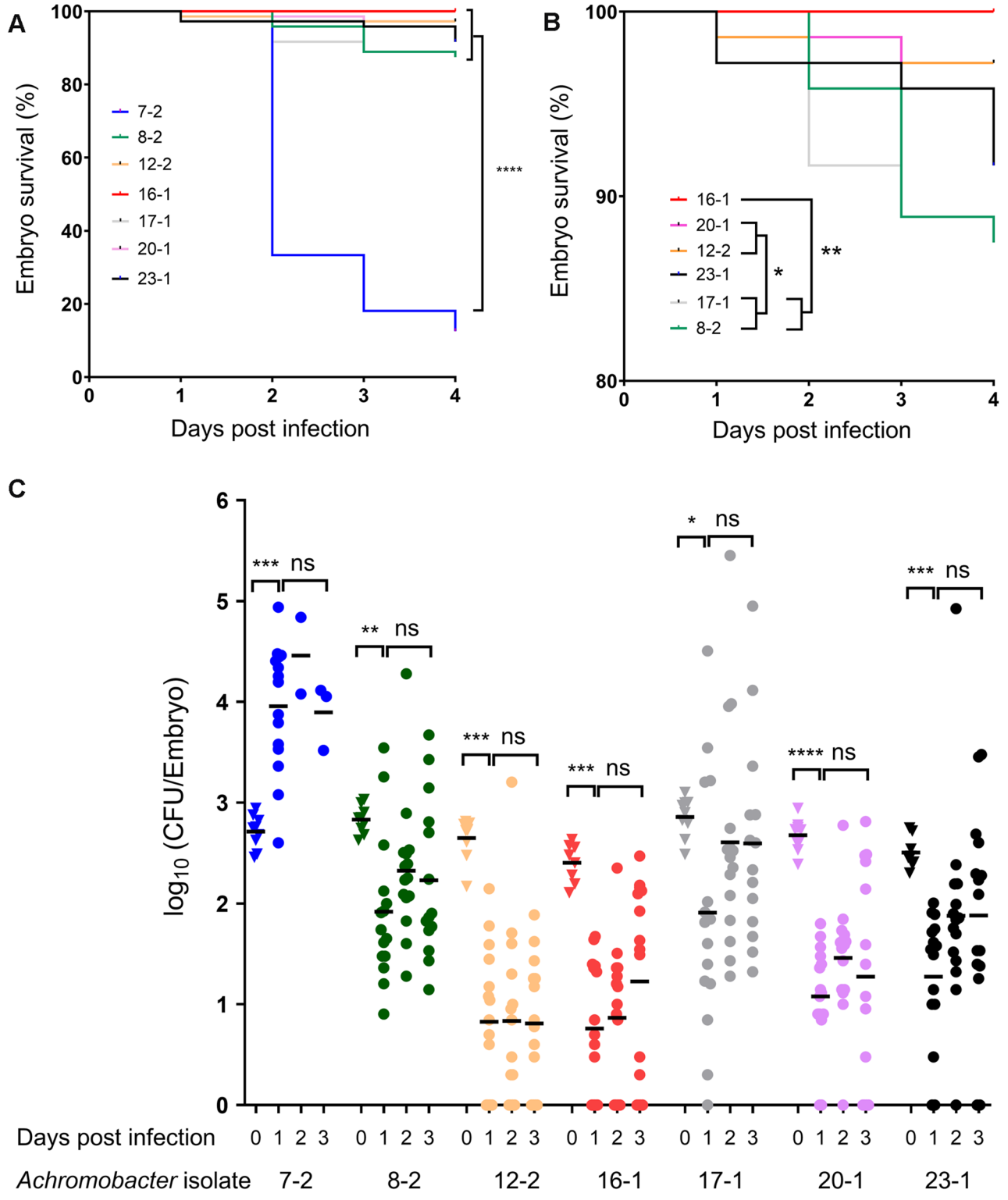

Fig. 1 Virulence of *Achromobacter* in zebrafish embryos. **A**, **B** Survival percentage of embryos injected intravenously with 7 *Achromobacter* isolates ($n=72$; 24 embryos per strain per experiment). Graph B shows an adapted scale of the 80–100% survival range indicated in graph A. Statistical analysis was performed using the log-rank (Mantel-Cox) test: ** = $P \leq 0.01$; **** = $P \leq 0.0001$. **C** Bacterial load. Each data point represents an individual embryo ($n=5$ per strain per experiment at 1, 2 and 3 dpi). Dead embryos are not represented. Horizontal black bars indicate the mean. Statistical analysis was performed using the non-parametric Kruskall-Wallis test with Dunn's post-hoc test comparing day 0 to day 1, and day 1 to day 3, * = $P \leq 0.05$; ** = ≤ 0.01; *** = $P \leq 0.001$; **** = $P \leq 0.0001$. **A-C** The average inoculum (T = 0, $n=3$ per strain per experiment) was: 7 – 2: 550 CFU; 8 – 2: 708 CFU; 12 – 2: 483 CFU; 16 – 1: 275 CFU; 17 – 1: 781 CFU; 20 – 1: 504 CFU; 23 – 1: 339 CFU

isolate 7 – 2 resulted in a significant 1.46 $\log_2$ increase at 1 dpi (Fig. 1C), in agreement with the high mortality rate triggered by this isolate (Fig. 1A). Due to the rapid death of the embryos infected with isolate 7 – 2, CFU counts at 2 and 3 dpi were performed on a few surviving embryos only. The high CFU counts ($\log_{10}$=4) at 2 and 3 dpi in these surviving embryos showed uncontrolled bacterial growth in all infected embryos, in agreement with the high mortality induced by this isolate. Strains 8 – 2, 17 – 1, and 23 – 1, which caused between 8.4% and 12.5% host mortality, showed a significant reduction in bacterial numbers at 1 dpi in most infected embryos (with respective mean $\log_2$ fold changes of 1.48, 1.5, and 1.96) but then the bacterial load remained constant over time until 3 dpi (mean $\log_2$ of 2.23, 2.60 and 1.90), sometimes reaching high numbers (Fig. 1C).

Importantly, almost all embryos (except 2 out of 15 embryos injected with strain 23 – 1) still contained live bacteria at 3 dpi. In contrast, in embryos injected with strains 12 – 2, 16 – 1, and 20 – 1, which induced the lowest mortality rates (< 3%), fewer bacteria persisted per embryo compared to the other strains (mean $\log_2$ of 0.8093, 1.227 and 1.274 at 3 dpi) with around 26% of embryos able to completely clear the bacteria. Overall, combining survival data and bacterial burden over time, strain 7 – 2 is highly virulent, strains 8 – 2, 17 – 1, and 23 – 1 are moderately virulent, while isolates 12 – 2, 16 – 1, and 20 – 1 show reduced virulence, but are persistent. Real time imaging further provided insight into the nature of the infection. After injection of around 200 CFU in the caudal vein (Fig. 2A), the most virulent strain 7 – 2 was observed in high bacterial numbers at different anatomical sites, including the vasculature, hind brain, central nervous system, and caudal hematopoietic tissue at 1 dpi (Fig. 2B-D), in agreement with high CFU counts and high mortality rates. In contrast, strain 16 – 1 was observed in low bacterial numbers from 1 to 3 dpi (Fig. 2E and F), in agreement with its reduced virulence. The bacteria were associated with macrophages (Fig. 2E-inset), as described in more detail below. The three moderately virulent strains induced local inflammation sites that persisted until 3 dpi (Fig. 3), while large bacterial numbers were observed in some embryos, presented as bacteraemia (Shown for isolate 23 – 1; Fig. 3 - Panel 2 dpi), in agreement with the occasional death observed for embryos injected with these strains at later time points.

Host immune response to infection

To gain more insight into the host immune response toward *Achromobacter* spp., we used RT qPCR to analyse changes in gene expression of several immune-related genes during infection with isolates 7 – 2 and 16 – 1, being the most and least virulent strains, respectively, of the panel. First, we analysed the expression of the major pro-inflammatory cytokine gene *il1b*, and the chemokine genes *cxcl8a* and *cxcl18b* (formerly *cxcl-c1c*). C*xcl18b* does not have any clear homologs in primate and rodent counterparts, but it has been suggested to be an important contributor to neutrophil chemotaxis in the inflammatory microenvironment and is involved in the chemotactic response towards neutrophils in zebrafish [33]. At 3 hpi, *il1b*, *cxcl8a* and *cxcl18b* expression was significantly increased in embryos infected with strain 7 – 2 (P = 0.0037, < 0.0001, and 0.014, respectively) and strain 16 – 1 (P = 0.001, < 0.0001, and 0.0003, respectively) compared to the PBS-injected control group. At this time point, no significant differences were detected between the two strains although *cxcl18b* expression was induced 2 $\log_2$ more after infection with the least virulent strain (16 – 1) (Fig. 4A). At 24 hpi, the relative fold-increase was between 4.6 $\log_2$ and 6.1 $\log_2$-fold for all three genes in embryos infected with strain 7 – 2 (P = < 0.0001, < 0.0001 and 0.0001, respectively) compared to the PBS-injected control, while embryos infected with strain 16 – 1 showed no significant difference in expression compared to PBS-injected control embryos. The gene expression data mirror the virulence levels observed for these strains (Fig. 1): while both strains induced the expression of cytokine genes at early time points, which is an expected host immune response after bacterial challenge, embryos infected with the virulent strain 7 – 2, but not strain 16 – 1, still expressed the analysed genes at significantly increased levels compared to PBS-injected embryos at 24 hpi.

We also analysed changes in expression of the metalloprotease 9 gene *mmp9*, which is usually upregulated during bacterial infections [34]. Although the increase in *mmp9* expression at 3 hpi was not significant, this gene was expressed to a higher level during persistent compared to acute infection (mean 1.7 $\log_2$ and 3.4 $\log_2$ respectively for 7 – 2 and 16 – 1 compared to PBS). At 24 hpi the virulent strain 7 – 2 significantly induced the expression of this metalloprotease gene (P = 0.0011, Fig. 4B).

The myeloid differentiation factor MYD88 is an important adaptor protein in interleukin 1 receptor (IL1R) and Toll-like receptor (TLR) signalling, while NFκB is an important transcription factor activated by TLR signalling and central to innate immunity. There are strong similarities between human and zebrafish TLR signalling pathways, and Myd88-dependent responses towards infection with *Salmonella enterica* serovar Typhimurium and *Mycobacterium marinum* in zebrafish embryos have been demonstrated [34]. Unexpectedly, *Achromobacter* infection did not result in significant changes in *myd88* and *nfkb2* expression in zebrafish embryos (Fig. 4B), suggesting that the TLR signalling pathway does not play a role in host defence against *Achromobacter*. The

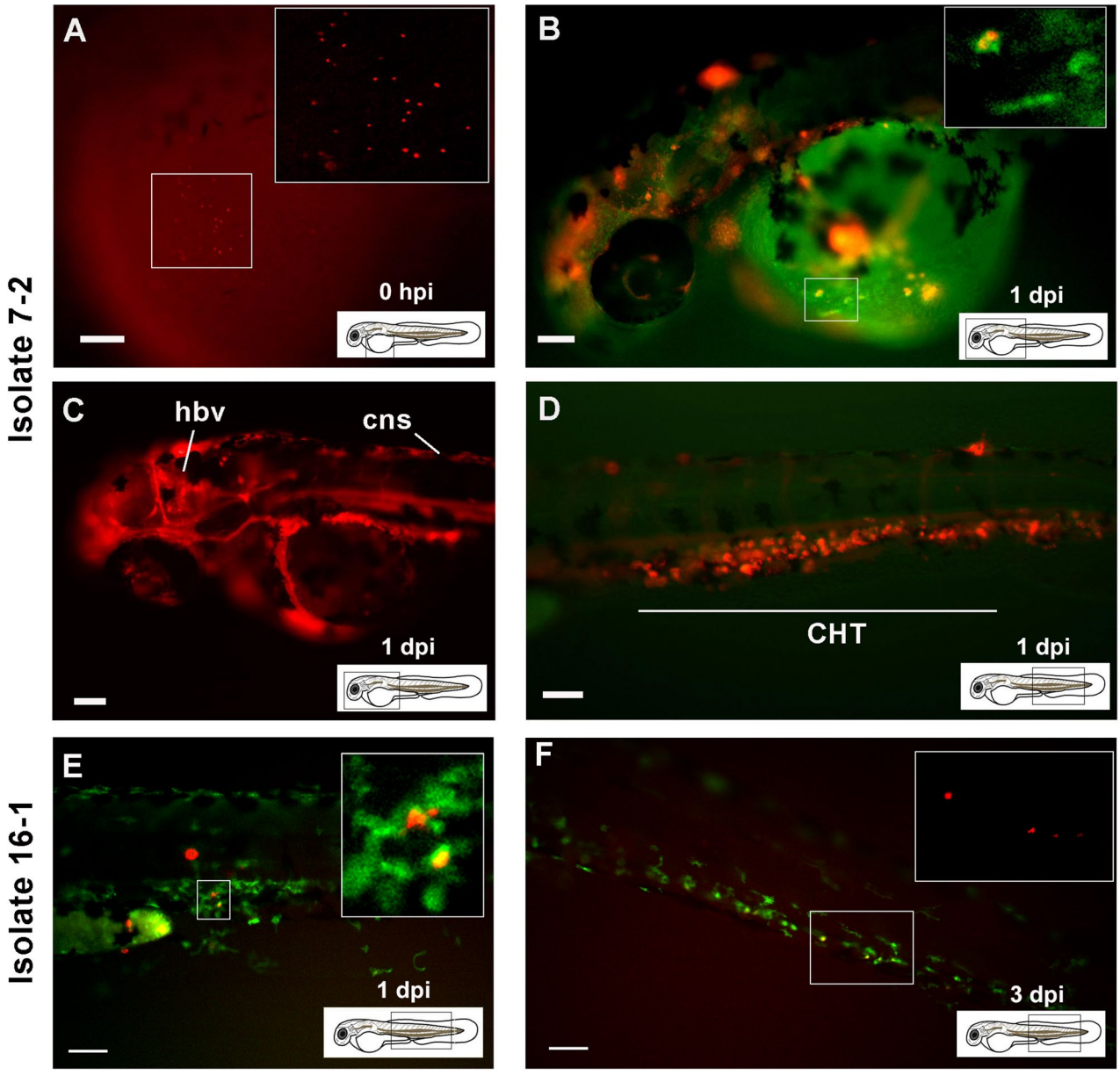

Fig. 2 Imaging of embryos infected with strains of high (7 – 2) and low (16 – 1) virulence. Tg(*mpeg1:eGFP-caax*)^{gl22} embryos, expressing GFP in macrophages (green channel), were injected with approximately 200 CFU of the isolates 7 – 2 and 16 – 1 expressing DSRed (red channel), and imaged using fluorescence microscopy. **A** Image of the yolk of an embryo immediately after injection in the caudal vein. **B-D** Three embryos injected with strain 7 – 2, imaged at 1 day post infection (dpi), showing high bacterial load in the vasculature, the hind brain ventricle (hbv), the central nervous system (cns), and the caudal haematopoietic tissue (CHT). Red channel (**C**) and overlay of red and green channels (**B**, **D**). The inset in (**B**) highlights a few bacteria associated with a macrophage. **E**, **F** Representative images of the tail region of an embryo injected with strain 16 – 1, imaged at 1 and 3 dpi, respectively, showing association of bacteria with macrophages (inset). Overlay of red and green channels. Scale bars: 50 µm. The embryo drawings indicate the imaged areas

expression of the myeloperoxidase (*mpx*) gene, which is expressed mainly in neutrophils, was not significantly changed during acute or persistent infection, although it was slightly downregulated at 24 h during acute infection.

To better understand the role of host immune cells during *Achromobacter* spp. infection, Tg(*mpx: eGFP*)^{i114} embryos with neutrophils expressing eGFP were injected with isolates 7 – 2 and 16 – 1. Neutrophils were quantified at 1, 2, and 3 dpi (Fig. 5). Although not significant, a minor reduction in the number of neutrophils was observed in embryos infected with strain 7 – 2 (average 141 ± 55 neutrophils per embryo, n = 18) in comparison to the noninfected control embryos at 1 dpi (average 171 ± 48 neutrophils per embryo, n = 17). Due to the rapid mortality induced by strain 7 – 2, later time points were not included. Three to 5 days post-fertilisation,

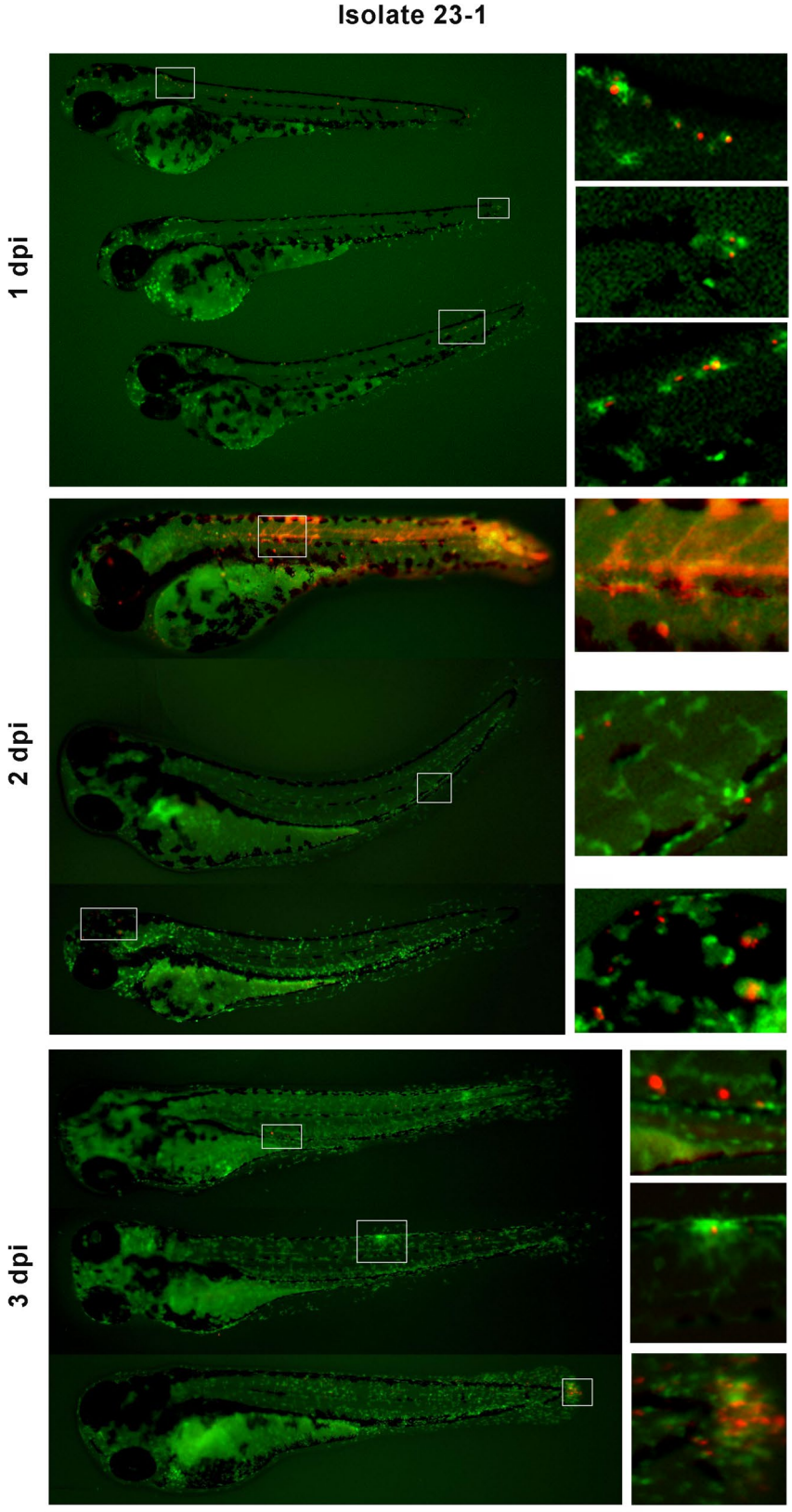

Fig. 3 The moderately virulent isolate 23 – 1 causes persistent infection and occasional bacteraemia. Tg(*mpeg1:eGFP-caax*)^{gl22} embryos (30 hpf), expressing GFP in macrophages (green channel) were injected with approximately 400 CFU of isolate 23 – 1 expressing DSRed (red channel), respectively, and imaged using fluorescence microscopy at 1, 2, and 3 dpi. The images show overlays of the green and red channels. Insets in each image represent bacteria, often associated with macrophages

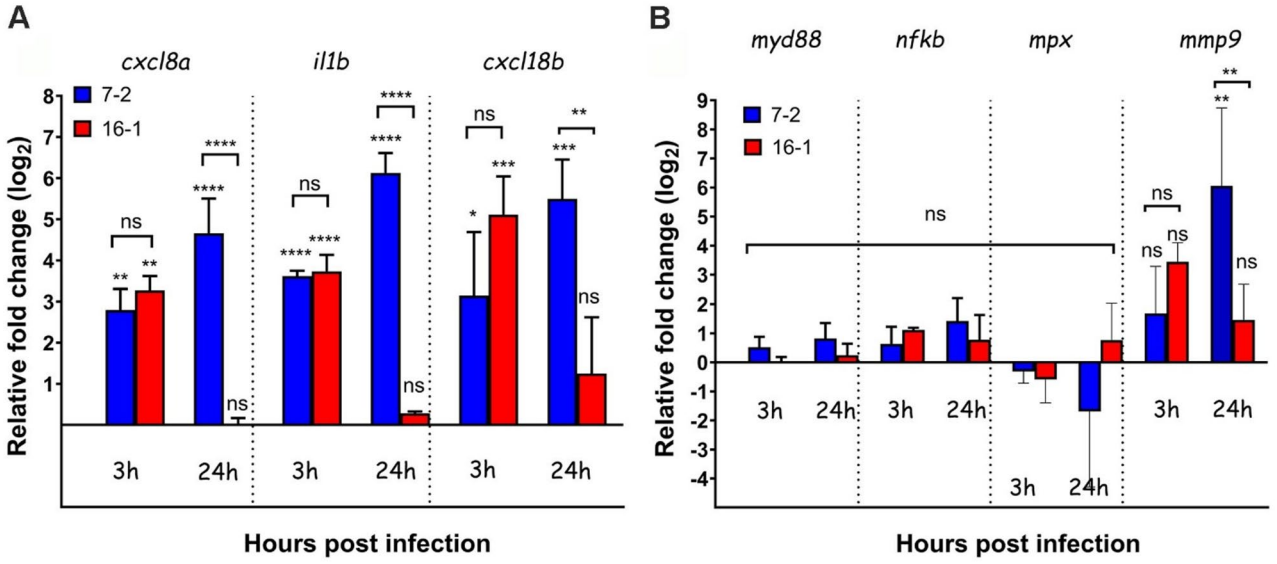

Fig. 4 Analysis of host gene expression with RT-qPCR. Mean relative changes in *il1b*, *cxcl8a and cxcl18b* (**A**) and *myd88*, *nfkb*, *mpx and mmp9* (**B**) gene expression in embryos injected with isolates 7 – 2 (blue bars) and 16 – 1 (red bars), normalized to a PBS-injected control group at each time point. Error bars represent the means ± SEM of three biological replicates. Statistical analysis was performed per gene, using a one-way ANOVA with Sidak's multiple comparison test; Asterisks above each bar indicate significance compared to the PBS control at each time point, significance between timepoints is indicated with a horizontal line. Ns = non-significant, * = $P \leq 0.05$; ** = $P \leq 0.01$; *** = $P \leq 0.001$; **** = $P \leq 0.0001$

haematopoiesis takes place in the caudal haematopoietic tissue (CHT) and neutrophils can be seen in the CHT as well as randomly migrating as described [35]. In infected embryos, a higher number of neutrophils can be observed in the CHT than in non-infected embryos (Fig. 5B), in line with emergency granulopoiesis. Overall, the number of neutrophils significantly increased over the course of infection in embryos infected with strain 16 – 1 compared with PBS-injected control embryos, suggesting emergency granulopoiesis in response to pro-inflammatory signals (Fig. 5).

We used fluorescence and confocal microscopy to further analyse the interaction between intravenously injected DSRed-expressing *Achromobacter* spp. and macrophages in Tg(*mpeg1:eGFP-caax*)^{gl22} zebrafish embryos which express GFP in the membrane fraction of macrophages. Confocal imaging revealed that intravenously injected bacteria were phagocytosed by macrophages (Fig. 6A, B). At later time points, bacteria were still found to be associated with macrophages and in greater numbers (Fig. 2B and E, Figs. 3 and 6C), suggesting that bacteria not only survive but also replicate in these immune cells. Bacteria were sometimes detected in GFP-negative cells during persistent infection at 3 dpi, suggesting that the bacteria can also survive in other cells.

To further analyse the role of macrophages during *Achromobacter* infection, we compared the behaviour of the isolate 16 – 1 in macrophage-proficient embryos and macrophage-depleted embryos (Pu.1 morphants) by using a Pu.1 morpholino strategy. Pu.1 morphants showed a significantly higher mortality than macrophage-proficient embryos after intravenous injection (Fig. 7A). This coincided with a strong significant increase in bacterial burden in Pu.1 morphants compared to macrophage-proficient embryos at 1 dpi (4.44 $\log_{10}$, Padj 0.0001) and 2 dpi (6.47 $\log_{10}$, Padj 0.0035). Real-time imaging confirmed the localisation of reduced numbers of bacteria of isolate 16 – 1 in macrophages of control embryos at 24 hpi (Fig. 7C), whereas Pu.1 morphants showed high bacterial burden at 24 hpi, with bacteria present in the vasculature (Fig. 7D). These findings demonstrate that macrophages play a host-protective role during persistent *Achromobacter* spp. infections. In agreement with the results obtained for strain 16 – 1, at 2 dpi, macrophage-deficient embryos infected with strain 7 – 2 died more rapidly than control embryos (84% and 47% mortality, respectively) indicating that macrophages also play a protective role during acute infection.

Discussion

This study showed that zebrafish embryos are an interesting additional model for studying the virulence of *Achromobacter* spp., specifically their interaction with the host innate immune system and the role of macrophages in real time. The strains used in this work have previously been shown to display differences in pathogenicity in *G. mellonella* larvae (host survival), cytotoxicity in human bronchial epithelial cells, and biofilm formation [32]. We earlier also showed that these strains displayed differences in pulmonary inflammation, survival, and bacterial

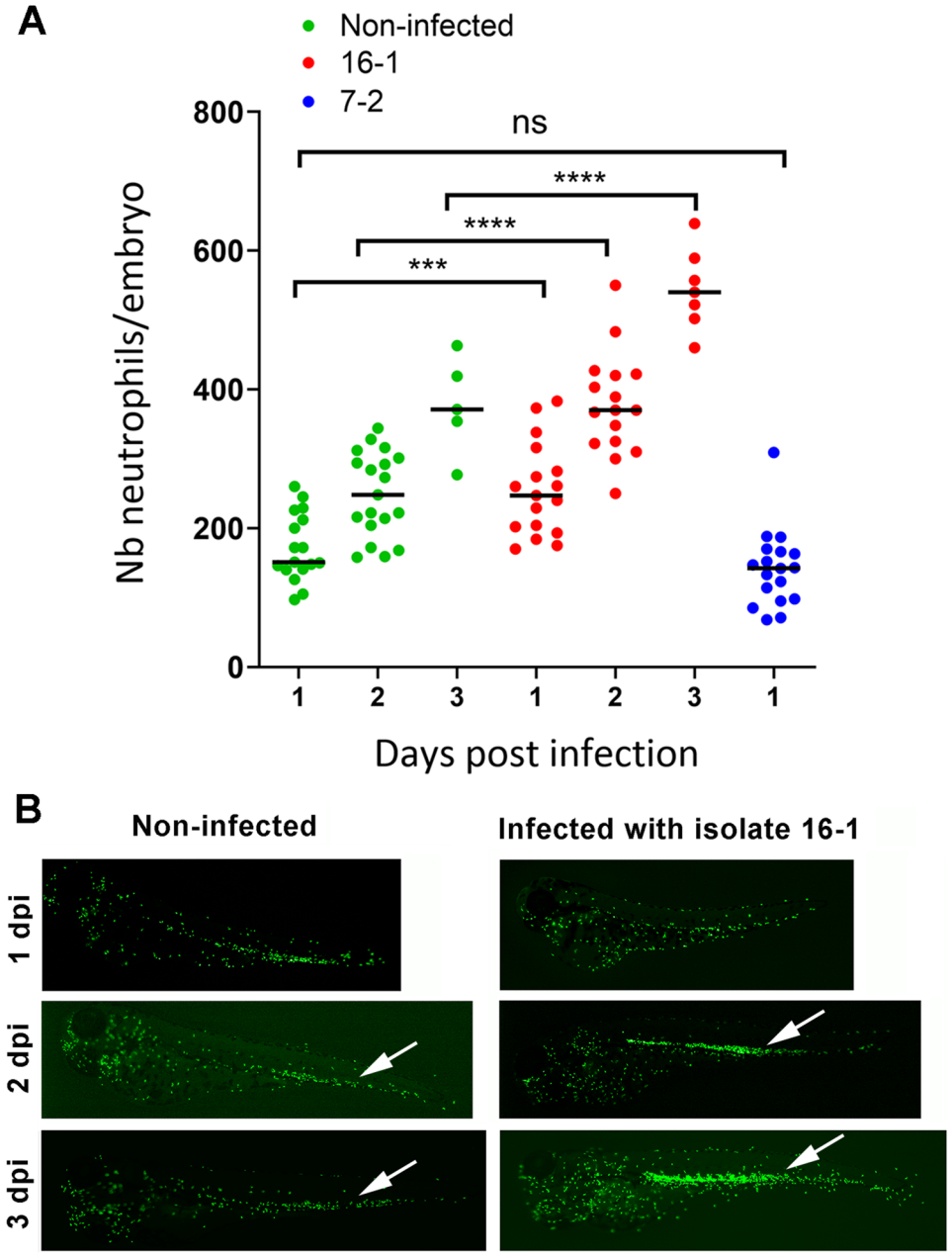

Fig. 5 Neutrophil numbers in Tg(*mpx: GFP*)^{i114} zebrafish embryos after intravenous injection of *Achromobacter* strains 7 – 2 and 16 – 1. **A** Neutrophil numbers were determined per embryo and indicated as individual dots. For strain 7 – 2, only 1 dpi counts are shown due to rapid embryo death. Two biological replicates are shown (total $n = 16$ to 19 embryos per strain per time point; the 3 dpi time point was performed only once $n = 5$ and 7, respectively). Statistical analysis was performed using a one-way ANOVA with Sidak's multiple comparisons test: ns = non-significant, ***=$P \leq 0.001$, ****= $P \leq 0.0001$. **B** Images of representative non-infected embryos and embryos injected with isolate 16 – 1, at 1, 2, and 3 dpi. Arrows indicate the caudal haematopoietic tissue (CHT)

load between WT and CFTR-knockout mice [14]. The zebrafish embryo model revealed infection outcomes among these seven *Achromobacter* spp. strains, ranging from lethal infection to low-burden, persistent infections. Among the seven isolates, one *A. xylosoxidans* strain caused rapidly fatal infection, three *A. xylosoxidans* strains showed an intermediate killing ability, and three *Achromobacter* spp. strains (not *A. xylosoxidans*) caused low mortality under the experimental conditions (Table 2). Although *A. xylosoxidans*, the species most frequently isolated in clinical settings, was the most virulent in our assay conditions, the low number of isolates in this study does not allow us to conclude that this species is most virulent in this model or, inversely, that

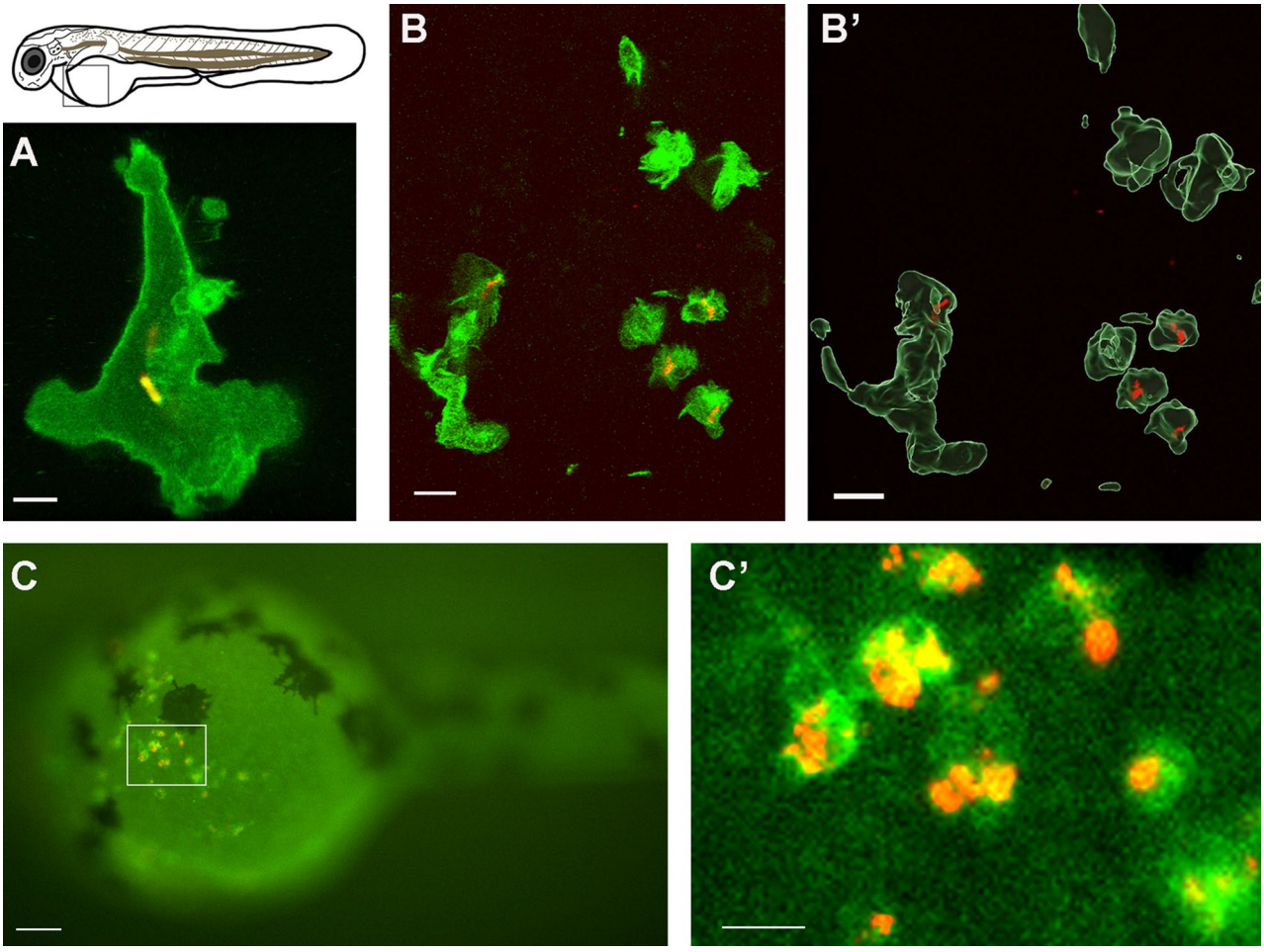

Fig. 6 *Achromobacter* is rapidly phagocytosed by macrophages and remains associated with macrophages at later time points. Tg(*mpeg1:eGFP-caax*)^{gl22} embryos, expressing GFP in macrophages (green channel) were injected with approximately 200 CFU of strain 7 – 2, expressing DSRed (red channel), and imaged over the yolk region. **A** Confocal image (z-stack of 14 images) of a macrophage with intracellular bacteria at 2.5 hpi. Overlay of red and green channels. Scale bar 4 µm. **B** Confocal image (z-stack of 71 images) of macrophages with intracellular bacteria, at 2.5 hpi. Overlay of red and green channels. Scale bar 20 µm. **B'** 3D surface rendering (Imaris) of the image shown in **B**. **C** Epi-fluorescence image of the yolk region of an infected embryo at 20 hpi. Scale bar 50 µm. The indicated region is shown enlarged in **C'** (increased intensity) showing bacteria associated with macrophages. Scale bar 10 µm

other species are avirulent. Overall, the virulence levels observed across the three models (*G. mellonella* larvae, mice, and zebrafish embryos) followed a similar trend in pathogenicity despite the biological and immunological differences among the hosts. For example, strain 7 – 2 displayed high virulence in *G. mellonella* and caused high mortality in both mice (75% WT; 100% CF) and zebrafish embryos (87.5%), indicating that this strain is highly virulent across multiple host models. Strains with low or no virulence in *G. mellonella*, such as 12 – 2 and 16 – 1, correspondingly showed low mortality in both zebrafish embryos (2.8% and 0%, respectively) and mice (0–25%), reflecting a reduced pathogenic potential. However, strain 8 – 2 showed high virulence in *G. mellonella* and mice but only intermediate effects in zebrafish embryos, whereas isolate 17 – 1 displayed reduced virulence in mice compared with intermediate virulence in the other two models. These findings support the concept that virulence is shaped by both universal determinants, which are effective across multiple hosts, and host-specific factors that differentially influence infection outcomes depending on the model. In addition, different bacterial species can widely vary in the degree of conservation of virulence mechanisms across multiple hosts: For *Burkholderia* for instance, virulence determinants were shown to be largely host-specific, with only a limited subset of the analysed factors contributing across multiple infection models [36], while for *Pseudomonas* virulence mechanisms were highly conserved between evolutionary divergent hosts [37].

No apparent correlation was found between virulence in any of the models (*G. mellonella*, mice and zebrafish) and the capacity of the strains to produce biofilms in vitro or cytotoxicity in bronchial epithelial cells [14, 31].

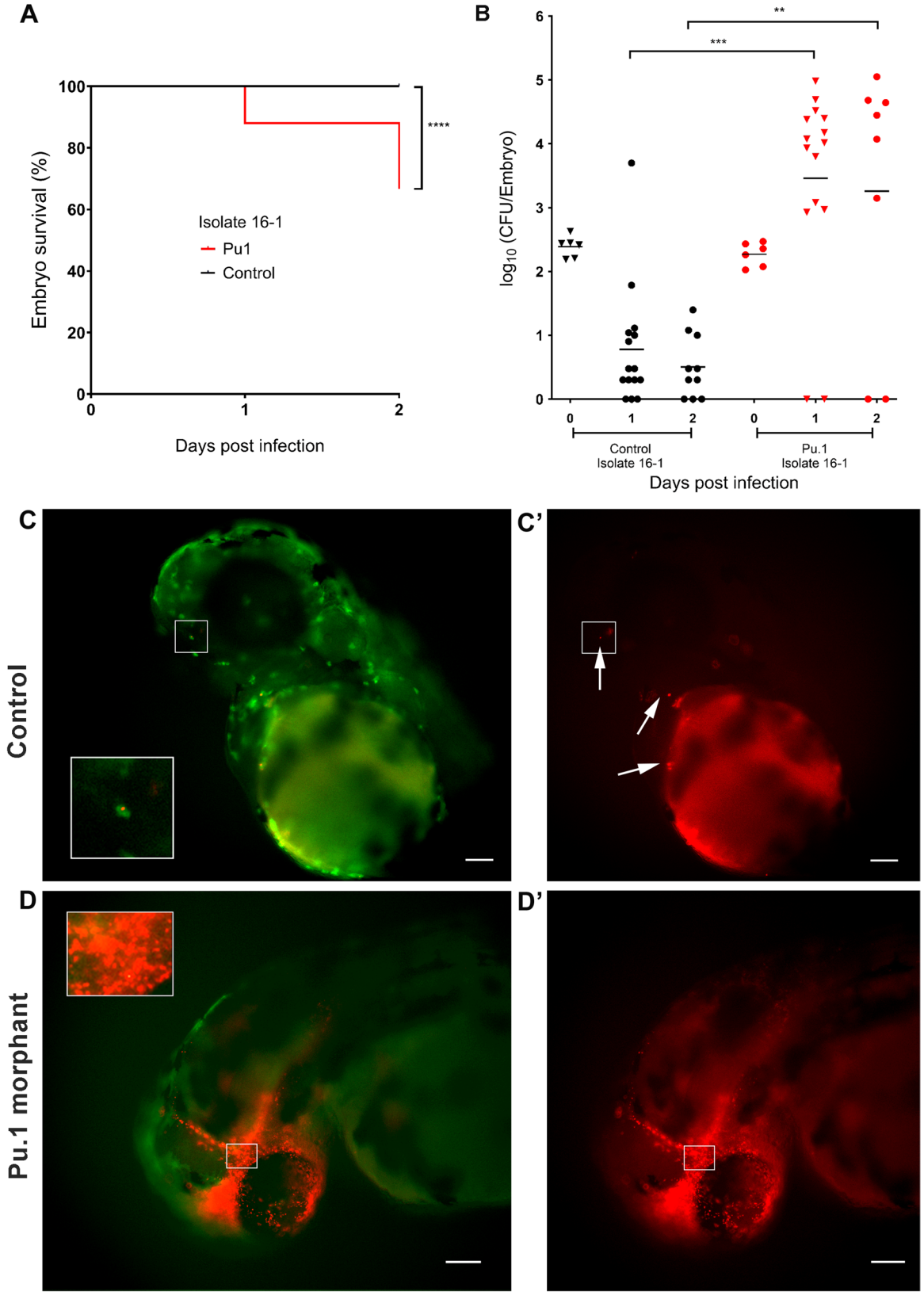

Fig. 7 (See legend on next page.)

(See figure on previous page.)

Fig. 7 Macrophages are important for host defence against *Achromobacter* infection. Tg(*mpeg1:eGFP-caax*)^{gl22} Pu.1 morphants and control embryos were intravenously injected with isolate 16 – 1 (inoculum: Control 260 ± 98 CFU; Pu.1 morphants 200 ± 78 CFU) in three biological replicates. **A** Survival analysis (Control, $n = 130$; Pu1, $n = 117$). Statistical analysis was performed using the Log rank (Mantel-Cox) test; **** = $P \leq 0.0001$. **B** Bacterial burden ($n = 5$ per experiment per group; the mean is indicated, with each data point representing an individual embryo). Statistical analysis was performed using the Kruskal-Wallis test with Dunn's multiple comparisons test, ** = $P \leq 0.01$; *** = $P \leq 0.001$. **C** Representative control embryo injected with isolate 16 – 1 expressing DSRed, 24 hpi. Overlay image of green (macrophages) and red (bacteria) channels. Inset: bacteria associated with a macrophage. **C'** Red channel of C showing few bacteria (Arrows). **D** Representative Pu.1 embryo injected with isolate 16 – 1 expressing DSRed, 24 hpi. Overlay of green (showing absence of macrophages) and red (bacteria) channels. Inset: High numbers of bacteria present in the blood circulation. **D'** Red channel of C highlighting bacterial load in the vasculature at 24 hpi. Scale bar: 50 µm

It would be interesting to determine a possible role in virulence in zebrafish embryos for the T3SS and the T3SS effectors AxoU and ArtA RTX [8, 12, 13]. Other bacterial factors that may contribute to differences in intracellular survival and host inflammatory responses include surface structures, stress response mechanisms, or toxins. Our previous genomic profiling of the isolates used in this study showed that 16 – 1, 12 – 2, and 20 – 1, the isolates inducing the lowest mortality, lack several genes associated with the ability to infect host cells, as well as genes involved in chemotactic movement, type III secretion system components, and protease production [14]. This might explain the comparatively low virulence observed for these isolates across the three infection models, although targeted functional studies will be required to confirm this link. In addition, factors important for fitness of environmental bacteria in competition with other soil organisms might be important non-classical virulence factors in eukaryotic organisms. As an example, the antifungal compound AFC, produced by *B. cenocepacia*, is a multi-host virulence factor [38, 39]. We have shown earlier that functional AFC is essential for the bacteria to cause acute infection in zebrafish embryos, while absence of this factor results in intracellular persistence only [40].

Based on our work with clinical and environmental *Burkholderia* strains [19, 41] and evidence that *Achromobacter* can evade intracellular degradation [8, 13], we used a relatively low inoculum of 400–500 CFU. This allowed studying a primary response of immune cells without overloading the embryo's circulation and masking differences in infection outcomes. Macrophages are the major cells that phagocytose microbes in the blood circulation of zebrafish embryos [42]. Like for *Burkholderia* spp., the ability of *Achromobacter* to delay and/or avoid elimination by macrophages and adopt an intracellular lifestyle likely contributes to their persistence following infection with a low bacterial inoculum. Strain 7 – 2 was able to cause acute infection even with a low inoculum, showing its ability to avoid elimination by host immune cells, and induce strong pro-inflammatory responses in the embryos that cannot be resolved. Our experiments do not exclude the possibility that a higher inoculum (> 1000 CFU), which would mimic bacteraemia with the ability of bacteria to replicate freely in the blood circulation in the absence of sufficient host immune cells to phagocytose them, would result in increased mortality with some of the isolates that showed low virulence. For *P. aeruginosa* and *S. aureus*, previously regarded as extracellular pathogens, higher inoculum doses (1000–3000 CFU) are typically needed to mimic acute infection; however, recent studies have demonstrated that *P. aeruginosa* and *S. aureus* are also able to survive and replicate within host cells, including in zebrafish embryos where they can cause persistent infection [43–47].

The strain that caused rapidly fatal infection in zebrafish embryos (isolate 7 – 2), has also been shown to be highly virulent in mice (including WT and CFTR mice) and *G. mellonella* larvae [14], a poor biofilm producer, and had intermediate cytotoxicity in bronchial epithelial cells (Table 2). The strong increase in *il1b*, *cxcl8*, *cxcl18b* and *mmp9* cytokine expression in embryos infected with isolate 7 – 2, specifically at later time points (24 hpi), further aligns with its acute infection profile and high mortality [33]. These findings parallel reports of increased pro-inflammatory cytokine production in severe *Achromobacter* spp. infections in murine models, where excessive inflammation contributes to tissue damage and mortality [15, 48]. In contrast to isolate 7 – 2, isolate 16 – 1 showed low pathogenicity in *G. mellonella* larvae and mouse models and was the least virulent in zebrafish embryos (Table 2). Embryos infected with strain 16 – 1 presented a transient induction of *il1b*, *cxcl8* and *cxcl18b* expression at early time points, accompanied by neutrophilic inflammation (Fig. 5), suggesting activation of emergency granulopoiesis to control the infection. Inflammatory signals have been shown to stimulate rapid myeloid cell production in zebrafish, as observed in models of *Shigella* infection where stem cell–driven granulopoiesis replenishes neutrophils, and via macrophage-derived Il1b, which regulates emergency myelopoiesis through the NF-κB and C/ebpβ pathways [49, 50]. Despite strong inflammatory signals, during acute infection with strain 7 – 2, neutrophil numbers were reduced compared to the non-infected control and to embryos infected with strain 16 – 1 (Fig. 5A). Currently, the mechanisms underlying the reduction in neutrophil numbers remain unclear. Possibly the extent of pro-inflammatory cytokine production induces apoptotic programs causing cell death of immune cells, and/or the production and release of pro-inflammatory mediators by neutrophils

to recruit and activate additional leukocytes results in exhausted neutrophils.

Cxcl18b is an additional fish-specific neutrophil chemoattractant, and its function depends on the chemokine receptor Cxcr2, but not on Cxcr1 and Cxcr4b [33]. Cxcl18b is a marker of inflammation since its transcription has been documented to be upregulated upon challenge with the fish pathogens *Edwardsiella tardi* and *M. marinum*, and with *S.* Typhimurium, as well as after treatment with toxic compounds [34, 51]. Therefore, it is not unexpected that this infection-response gene is upregulated after challenge inoculation with *Achromobacter*. It is interesting, however, that *cxcl18b* expression, as well as the expression of the metalloprotease gene *mmp9*, is transiently increased at an early time point to higher levels during persistent non-fatal infection than during acute pro-inflammatory infection, even though the difference is not significant. It would be interesting to further analyse potential differences in early pro-inflammatory host responses after challenge inoculation with pathogens that are known to cause different infection profiles. In addition, the expression of both *cxcl18b* and *mmp9* has been shown to be dependent on a functional Myd88 pathway [34], suggesting that the Myd88 signaling pathway must be activated during *Achromobacter* infection.

Not much is known about the implication of the TLR-MYD88 signalling pathway during infection of *Achromobacter*. Therefore, we analysed the expression of *myd88* and *nfkb2* during acute and persistent infection. While the expression of these genes has been shown to be upregulated after infection of zebrafish embryos with *S.* Typhimurium [34], acute infection caused by *Achromobacter* did not result in significant changes in *myd88* and *nfkb2* gene expression (Fig. 4B), which suggests that TLR signalling does not play a role during *Achromobacter* infection. However, the TLR signalling pathway must be activated, since *il1b* expression, which we found to be increased during infection, depends largely on transcriptional activation by NfkB. In addition, as described above, *cxcl18b* has equally been described to depend on Myd88 signaling. Our data therefore suggest that de novo synthesis of Myd88 and Nfkb2 is not required during *Achromobacter* infection. Other intracellular immune defence pathways may contribute to the strong host response during infection with strain 7 – 2. In particular, *Achromobacter* has been shown to activate the inflammasomes Nod-like receptor (NLR) family CARD domain-containing protein 4 (NLRC4) and NLR family pyrin domain containing 3 (NLRP3) in macrophages, resulting in Caspase-1 cleavage and IL-1β release [8].

A key finding from our study is the critical role of macrophages in controlling bacterial growth and limiting infection severity caused by a strain with low virulence (16 – 1). In macrophage-depleted zebrafish embryos, infection with strain 16 – 1 led to a significantly higher bacterial burden and increased host mortality than it did in macrophage-proficient embryos, underscoring the essential role of these immune cells in defence against *Achromobacter* spp. Using confocal imaging, bacteria were detected inside macrophages during persistent and acute infection, also at later time points after infection. These observations are consistent with in vitro studies showing that *Achromobacter* spp. can survive within cultured macrophages, suggesting that these immune cells play a detrimental role for the host by providing a niche for bacterial persistence and replication [8, 13]. Our imaging data suggest that strain 7 – 2 is also able to survive and replicate intracellularly (Fig. 6C), and that infected macrophages are not killed through cell death mechanisms. While this study was focussed on determining whether the zebrafish is a suitable model to study virulence of *Achromobacter* spp., further studies should be focussed on analysing correlations between cytotoxicity in bronchial epithelial cells and macrophages in vitro, and virulence in the zebrafish model, with a possible role for the T3SS and the T3SS effectors AxoU and ArtA RTX [8, 12, 13]. In addition, here we did not analyse the persistent character of the bacteria beyond 5 days post fertilisation, but it would be interesting to study bacterial persistence for longer periods of time, especially considering the importance of chronic lung infections in CF.

The zebrafish embryo model has several limitations, including the absence of an adaptive immune system, impossibility to mimic respiratory infections, and differences in physiology compared to mammals. However, the transparent nature of the embryos and the similarity of their innate immune system to that of mammals make it a powerful model to visualise infections in real time, to dissect host-pathogen mechanisms in the context of an innate immune response, and study immune cell/bacteria interactions in large detail, which is unparalleled in other models. They provide a model for studying the bacterial and host factors that are involved in persistent and acute infections. The strains used in this study were isolated from CF patients. They are virulent in CFTR-proficient mice and zebrafish, in agreement with the ability of *Achromobacter* spp. to cause nosocomial non-CF infections. It will be interesting to analyse a larger panel of strains comparing CF, non-CF and environmental isolates for virulence in zebrafish.

Conclusions

Our study shows that zebrafish embryos are a powerful in vivo model for the studying the pathogenicity of *Achromobacter* spp. and their ability to evade host killing in the context of an innate immune system. Our results demonstrate an important role for macrophages in controlling

Achromobacter infection, yet these opportunistic bacteria are able to survive and even replicate in macrophages in a strain-dependent manner. This infection model will be useful in identifying novel therapeutic strategies to combat infections in vulnerable people, including the screening of compounds targeting bacterial persistence and the in vivo evaluation of antibiotic efficacy within a physiologically relevant host immune environment.

Acknowledgements
The authors wish to thank the Cystic Fibrosis Centre at Verona Hospital for the bacterial strains provided. This work is part of the PhD thesis of Giulia Maria Saitta, which was deposited online by the University of Verona in 2025 (https://iris.univr.it/handle/11562/1161867). The present manuscript includes the data described on pages 80-99 of the thesis.

Authors' contributions
Experiments were conceived by GMS, ACV, and AS, and performed by GMS, JB, QM, EAO, and ACV. JB maintained the ZF facility. GMS, ACV, and JB analysed the data. CS, ACV, and DOC obtained financing. AS, MB, MML, CS, and ACV supervised the project. PM, MML, and CS provided resources. GMS drafted the manuscript. ACV and DOC extensively reviewed and revised the manuscript. All authors reviewed and approved the submitted manuscript.

Funding
Univ Montpellier (AAP Soutien à la recherche 2020), Nîmes Métropole, INSERM, and the Nimes University Hospital financed the VBIC zebrafish facility. Research at VBIC is financed by institutional grants from the University of Montpellier and Inserm. The Verona team is financed by Prof. Signoretto's university grants. GMS was supported by a PhD grant from the University of Verona, and an Erasmus + fellowship to visit VBIC. MQ was supported by a China Scholarship Council grant from the Ministry of Education of the P.R. China. EAO was supported by a scholarship awarded by the Brazilian National Council for Scientific and Technological Development (CNPq).

Data availability
All data supporting the findings of this study are available within the paper.

Declarations

Ethics approval and consent to participate
The zebrafish facility of VBIC (Bacterial Virulence and Chronic infections) received approval from the Direction Départementale de la Protection des Populations du Gard (ID 30-189-4). Infection experiments were ended 5 days post-fertilisation and were not classified as animal experimentation under the 2010/63/EU Directive, and therefore they did not require authorisation from the ethical committee.

Consent for publication
Not applicable.

Competing interests
The authors declare no competing interests.

Author details
[1]Department of Diagnostics and Public Health, Microbiology Section, University of Verona, Verona 37134, Italy
[2]VBIC, Univ Montpellier, INSERM, CHU Nîmes, Nîmes, France
[3]Department of Immunology and Microbiology, School of Basic Medical Sciences, Key Laboratory of Traditional Chinese Medicine Toxicology in Forensic Medicine, Guizhou Education Department, Guizhou University of Traditional Chinese Medicine, Guiyang, China
[4]Department of Veterinary Medicine, LISASC- Laboratórios Integrados de Sanidade Animal e Saúde Coletiva, Federal University of Lavras, Lavras, Brazil
[5]Cystic Fibrosis Centre, Azienda Ospedaliera Universitaria Integrata Verona, Piazzale A. Stefani 1, Verona 37126, Italy
[6]Departemental Clinical Genetics Unit, University of Verona, Verona 37134, Italy

Received: 17 December 2025 / Accepted: 18 May 2026
Published online: 29 May 2026

References

1. Amoureux L, Bador J, Verrier T, Mjahed H, De Curraize C, Neuwirth C. *Achromobacter xylosoxidans* is the predominant *Achromobacter* species isolated from diverse non-respiratory samples. Epidemiol Infect. 2016;144:3527–30. https://doi.org/10.1017/S0950268816001564.
2. Neidhöfer C, Berens C, Parčina M. An 18-year dataset on the clinical incidence and MICs to antibiotics of *Achromobacter* spp. (labeled biochemically or by MALDI-TOF MS as *A. xylosoxidans*), largely in patient groups other than those with CF. Antibiotics. 2022;11(3):311. https://doi.org/10.3390/antibiotics11030311.
3. Firmida MC, Pereira RHV, Silva EASR, Marques EA, Lopes AJ. Clinical impact of *Achromobacter xylosoxidans* colonization/infection in patients with cystic fibrosis. Braz J Med Biol Res. 2016;49(4). https://doi.org/10.1590/1414-431X20155097.
4. Rønne Hansen C, Pressler T, Høiby N, Gormsen M. Chronic infection with *Achromobacter xylosoxidans* in cystic fibrosis patients; a retrospective case control study. J Cyst Fibros. 2006;5:245–51. https://doi.org/10.1016/j.jcf.2006.04.002.
5. Hansen CR, Pressler T, Nielsen KG, Jensen P, Bjarnsholt T, Høiby N. Inflammation in *Achromobacter xylosoxidans* infected cystic fibrosis patients. J Cyst Fibros. 2010;9:51–8. https://doi.org/10.1016/j.jcf.2009.10.005.
6. Bruscia EM, Bonfield TL. Cystic fibrosis lung immunity: the role of the macrophage. J Innate Immun. 2016. https://doi.org/10.1159/000446825. 8:550 – 63.
7. Nielsen SM, Nørskov-Lauritsen N, Bjarnsholt T, Meyer RL. *Achromobacter* species isolated from cystic fibrosis patients reveal distinctly different biofilm morphotypes. Microorganisms. 2016;4:33. https://doi.org/10.3390/MICROORGANISMS4030033.
8. Turton K, Parks HJ, Zarodkiewicz P, Hamad MA, Dwane R, Parau G, et al. The *Achromobacter* type 3 secretion system drives pyroptosis and immunopathology via independent activation of NLRC4 and NLRP3 inflammasomes. Cell Rep. 2023;42:113012. https://doi.org/10.1016/j.celrep.2023.113012.
9. Le Goff M, Vastel M, Lebrun R, Mansuelle P, Diarra A, Grandjean T, et al. Characterization of the *Achromobacter xylosoxidans* type VI secretion system and its implication in cystic fibrosis. Front Cell Infect Microbiol. 2022;12:859181. https://doi.org/10.3389/FCIMB.2022.859181.
10. Veschetti L, Sandri A, Johansen HK, Lleò MM, Malerba G. Hypermutation as an evolutionary mechanism for *Achromobacter xylosoxidans* in cystic fibrosis lung infection. Pathogens. 2020;9(2):72. https://doi.org/10.3390/pathogens9020072.
11. Wills BM, Garai P, Riegert MO, Sanchez FT, Pickrum AM, Frank DW, et al. Identification of virulence factors involved in a murine model of severe *Achromobacter xylosoxidans* infection. Infect Immun. 2023;91:e00037–23. https://doi.org/10.1128/IAI.00037-23.
12. Pickrum AM, DeLeon O, Dirck A, Tessmer MH, Riegert MO, Biller JA, et al. *Achromobacter xylosoxidans* cellular pathology is correlated with activation of a type III secretion system. Infect Immun. 2020;88:e00136–20. https://doi.org/10.1128/IAI.00136-20.
13. Pickrum AM, Riegert MO, Wells C, Brockman K, Frank DW. The in vitro replication cycle of *Achromobacter xylosoxidans* and identification of virulence genes associated with cytotoxicity in macrophages. Microbiol Spectr. 2022;10:e0208322. https://doi.org/10.1128/spectrum.02083-22.
14. Sandri A, Saitta GM, Veschetti L, Boschi F, Passarelli Mantovani R, Carelli M, et al. In Vivo Inflammation caused by *Achromobacter* spp. cystic fibrosis clinical isolates exhibiting different pathogenic characteristics. Int J Mol Sci. 2023;24:7432. https://doi.org/10.3390/IJMS24087432.
15. Elias-Oliveira J, Prado MKB, Souza COS, Pastore MR, Ramos SG, Costa Darini AL, et al. CD14 signaling mediates lung immunopathology and mice mortality induced by *Achromobacter xylosoxidans*. Inflamm Res. 2022;71:1535–46. https://doi.org/10.1007/s00011-022-01641-8.
16. Yoshida N, Domart MC, Peddie CJ, Yakimovich A, Mazon-Moya MJ, Hawkins TA, et al. The zebrafish as a novel model for the in vivo study of *Toxoplasma gondii* replication and interaction with macrophages. Dis Model Mech. 2020;13:dmm043091. https://doi.org/10.1242/DMM.043091.

17. Liu J, Yuan X, Fan C, Ma G. Application of the zebrafish model in human viral research. Virus Res. 2024;341:199327. https://doi.org/10.1016/J.VIRUSRES.2024.199327.
18. Gomes MC, Mostowy S. The Case for Modeling Human Infection in Zebrafish. Trends Microbiol. 2020;28:10–8. https://doi.org/10.1016/j.tim.2019.08.005.
19. Mesureur J, Feliciano JR, Wagner N, Gomes MC, Zhang L, Blanco-Gonzalez M, et al. Macrophages, but not neutrophils, are critical for proliferation of *Burkholderia cenocepacia* and ensuing host-damaging inflammation. PLoS Pathog. 2017;13:1–29. https://doi.org/10.1371/journal.ppat.1006437.
20. Clatworthy AE, Lee JSW, Leibman M, Kostun Z, Davidson AJ, Hung DT. *Pseudomonas aeruginosa* infection of zebrafish involves both host and pathogen determinants. Infect Immun. 2009;77:1293–303. https://doi.org/10.1128/IAI.01181-08.
21. Prajsnar TK, Cunliffe VT, Foster SJ, Renshaw SA. A novel vertebrate model of *Staphylococcus aureus* infection reveals phagocyte-dependent resistance of zebrafish to non-host specialized pathogens. Cell Microbiol. 2008;10:2312–25. https://doi.org/10.1111/j.1462-5822.2008.01213.x.
22. Renshaw SA, Trede NS. A model 450 million years in the making: Zebrafish and vertebrate immunity. Dis Model Mech. 2012;5:38–47. https://doi.org/10.1242/dmm.007138.
23. EllettF, Pase L, Hayman JW, Andrianopoulos A, Lieschke GJ. *mpeg1* promoter transgenes direct macrophage-lineage expression in zebrafish. Blood. 2011;117(4):e49-e56. https://doi.org/10.1182/blood-2010-10-314120.
24. Veschetti L, Boaretti M, Saitta GM, Passarelli Mantovani R, Lleò MM, Sandri A, et al. *Achromobacter* spp. prevalence and adaptation in cystic fibrosis lung infection. Microbiol Res. 2022;263:127140. https://doi.org/10.1016/j.micres.2022.127140.
25. Vergunst AC, Meijer AH, Renshaw SA, O'Callaghan D. *Burkholderia cenocepacia* creates an intramacrophage replication niche in zebrafish embryos, followed by bacterial dissemination and establishment of systemic infection. Infect Immun. 2010;78:1495–508. https://doi.org/10.1128/IAI.00743-09.
26. Mesureur J, Vergunst AC. Zebrafish embryos as a model to study bacterial virulence. Methods Mol Biol. 2014;1197:41–66. https://doi.org/10.1007/978-1-4939-1261-2.
27. Mocho JP, Lang F, Valentin G, Bedu S, McKimm R, Ramos J, Saavedra Torres Y, Wheatley SE, Higgins J, Millington ME, Lundegaard PR, Chamorro Valverde R, Jenčič V, von Krogh K. A multi-site-assessment of anesthetic overdose, hypothermic shock, and electrical stunning as methods of euthanasia for zebrafish (*Danio rerio*) embryos and larvae. Biology (Basel). 2022;11:546. https://doi.org/10.3390/biology11040546.
28. Hsu K, Traver D, Kutok JL, Hagen A, Liu TX, Paw BH, et al. The *pu.1* promoter drives myeloid gene expression in zebrafish. Blood. 2004;104:1291–7. https://doi.org/10.1182/BLOOD-2003-09-3105.
29. Su F, Juarez Ma, Cooke CL, Lapointe L, Shavit Ja, Yamaoka JS, et al. Differential regulation of primitive myelopoiesis in the zebrafish by Spi-1/Pu.1 and C/ebp1. Zebrafish. 2007;4:187–99. https://doi.org/10.1089/zeb.2007.0505.
30. Saitta GM, Veschetti L, Feletti R, Sandri A, Boaretti M, Melotti P, et al. Development of a simple and accurate molecular protocol using 16SrRNA for species-specific identification of *Achromobacter* spp. Pathogens. 2025;14(3):271. https://doi.org/10.3390/pathogens14030271.
31. Veschetti L, Sandri A, Patuzzo C, Melotti P, Malerba G, Lleo MM. Genomic characterization of *Achromobacter* species isolates from chronic and occasional lung infection in cystic fibrosis patients. Microb Genom. 2021;7:606. https://doi.org/10.1099/mgen.0.000606.
32. Sandri A, Veschetti L, Saitta GM, Passarelli Mantovani R, Carelli M, Burlacchini G, et al. *Achromobacter* spp. adaptation in cystic fibrosis infection and candidate biomarkers of antimicrobial resistance. Int J Mol Sci. 2022;23(16):9265. https://doi.org/10.3390/ijms23169265.
33. Torraca V, Otto NA, Tavakoli-Tameh A, Meijer AH. The inflammatory chemokine Cxcl18b exerts neutrophil-specific chemotaxis via the promiscuous chemokine receptor Cxcr2 in zebrafish. Dev Comp Immunol. 2017;67:57–65. https://doi.org/10.1016/J.DCI.2016.10.014.
34. van der Vaart M, van Soest JJ, Spaink HP, Meijer AH. Functional analysis of a zebrafish *myd88* mutant identifies key transcriptional components of the innate immune system. Dis Model Mech. 2013;6:841–54. https://doi.org/10.1242/dmm.010843.
35. Harvie EA, Huttenlocher A. Neutrophils in host defense: new insights from zebrafish. J Leukoc Biol. 2015;98:523–37. https://doi.org/10.1189/jlb.4MR1114-524R.
36. Uehlinger S, Schwager S, Bernier SP, Riedel K, Nguyen DT, Sokol PA, Eberl L. Identification of specific and universal virulence factors in *Burkholderia cenocepacia* strains by using multiple infection hosts. Infect Immun. 2009;77:4102–10. https://doi.org/10.1128/IAI.00398-09.
37. Mahajan-Miklos S, Tan M-W, Rahme LG, Ausubel FM. Molecular mechanisms of bacterial virulence elucidated using a *Pseudomonas aeruginosa-Caenorhabditis elegans* pathogenesis model. Cell. 1999;96:47–56. https://doi.org/10.1016/S0092-8674(00)80958-7.
38. Subramoni S, Nguyen DT, Sokol PA. *Burkholderia cenocepacia* ShvR-regulated genes that influence colony morphology, biofilm formation, and virulence. Infect Immun. 2011;79:2984–97. https://doi.org/10.1128/IAI.00170-11.
39. Thomson ELS, Dennis JJ. Common duckweed (*Lemna minor*) is a versatile high-throughput infection model for the *Burkholderia cepacia* Complex and other pathogenic bacteria. PLoS ONE. 2013;8:e80102. https://doi.org/10.1371/journal.pone.0080102.
40. Gomes M, Tasrini Y, Subramoni S, Agnoli K, Feliciano J, Eberl L, Sokol P, O'Callaghan D, Vergunst A. The *afc* antifungal activity cluster, which is under tight regulatory control of ShvR, is essential for transition from intracellular persistence of *Burkholderia cenocepacia* to acute pro-inflammatory infection. PLoS Pathog. 2018;14:e1007473. https://doi.org/10.1371/journal.ppat.1007473.
41. Gigan J, Boyer J, Moulin L, Vergunst AC. Analysis of the potential of environmental *Burkholderia sensu lato* isolates to cause infection in a zebrafish embryo model. BioRxiv. 2024. https://doi.org/10.1101/2024.12.26.630235.
42. LeGuyader D, Redd MJ, Colucci-Guyon E, Murayama E, Kissa K, Briolat V, et al. Origins and unconventional behavior of neutrophils in developing zebrafish. Blood. 2008;111:132–41. https://doi.org/10.1182/blood-2007-06-095398.
43. Pont S, Nilly F, Berry L, Bonhoure A, Alford MA, Louis M, et al. Intracellular *Pseudomonas aeruginosa* persist and evade antibiotic treatment in a wound infection model. PLoS Pathog. 2025;21(2):e1012922. https://doi.org/10.1371/journal.ppat.1012922.
44. Resko ZJ, Suhi RF, Thota AV, Kroken AR. Evidence for intracellular *Pseudomonas aeru*ginosa. J Bacteriol. 2024;206(5):e0010924. https://doi.org/10.1128/jb.00109-24.
45. Hajjar H, Berry L, Wu Y, Touqui L, Vergunst AC, Blanc-Potard A-B. Contribution of intramacrophage stages to *Pseudomonas aeruginosa* infection outcome in zebrafish embryos: insights from *mgtC* and *oprF* mutants. Sci Rep. 2024;14:6297. https://doi.org/10.1038/s41598-024-56725-8.
46. Fraunholz M, Sinha B, Mcgavin MJ, Fitzgerald R, Institute R. Intracellular *Staphylococcus aureus*: live-in and let die. Front Cell Infect Microbiol. 2012;2:43. https://doi.org/10.3389/fcimb.2012.00043.
47. Lopes IR, Alcantara LM, Silva RJ, Josse J, Vega EP, Cabrerizo AM, et al. Microscopy-based phenotypic profiling of infection by *Staphylococcus aureus* clinical isolates reveals intracellular lifestyle as a prevalent feature. Nat Commun. 2022;13:7174. https://doi.org/10.1038/s41467-022-34790-9.
48. Billiot CE, Novak L, McDaniel MS, Lindgren NR, Swords WE. Pathogenesis of *Achromobacter xylosoxidans* respiratory infections: colonization, persistence, and transcriptome profiling in synthetic cystic fibrosis sputum medium. Infect Immun. 2023;91:e00416–23. https://doi.org/10.1128/iai.00416-23.
49. Willis AR, Torraca V, Gomes MC, Shelley J, Mazon-moya M. *Shigella*-induced emergency granulopoiesis protects zebrafish larvae from secondary infection. mBio. 2018;9:e00933–18. https://doi.org/10.1128/mBio.00933-18.
50. Wei Z, Li C, Zhang Y, Lin C, Zhang Y, Shu L, Luo L, Zhuo J, Li L. Macrophage-derived IL-1β regulates emergency myelopoiesis via the NF-κB and C/ebpβ in zebrafish. J Immunol. 2020;205:2694–706. https://doi.org/10.4049/jimmunol.2000473.
51. Stockhammer OW, Zakrzewska A, Hegedus Z, Spaink HP, Meijer AH. Transcriptome profiling and functional analyses of the zebrafish embryonic innate immune response to Salmonella infection. J Immunol. 2009;182:5641–53. https://doi.org/10.4049/jimmunol.0900082.

Publisher's note